Available online at www.sciencedirect.com
SCIENCE DIRECT®
Chemical Physics Letters 422 (2006) 358–362
CHEMICAL PHYSICS LETTERS
www.elsevier.com/locate/cplett

Structural optimization of silver clusters from Ag_{61} to Ag_{120} by dynamic lattice searching method

Huan Zhan [a], Longjiu Cheng [a], Wensheng Cai [a,b], Xueguang Shao [a,b,*]

[a] Department of Chemistry, University of Science and Technology of China, Hefei, Anhui 230026, PR China
[b] Department of Chemistry, Nankai University, Tianjin 300071, PR China

Received 27 December 2005; in final form 22 February 2006
Available online 2 March 2006

Abstract

Structures of silver clusters from Ag_{61} to Ag_{120} were optimized with an unbiased global optimization algorithm named dynamic lattice searching (DLS). The interaction among silver atoms is modeled by the Gupta potential. New global minima of Ag_{79} and Ag_{80} were found. The results show that there are two magic number clusters Ag_{75} and Ag_{101} from Ag_{61} to Ag_{120}. Most of the clusters in the studied sizes have decahedral motifs, however, there are 9 clusters with non-decahedral pattern between the two neighboring magic numbers. These results might help us understand the growth rules of medium sized silver clusters.

1. Introduction

In recent years, the study of clusters has evoked great interest in scientists because they provide a bridge between molecules and the bulk materials. It has been found that clusters often display unique chemical and physical properties that are quite different from molecules and bulk materials [1]. Many experimental [2] and theoretical [3–5] investigations have been done on clusters. Generally, clusters can be divided into metal clusters and non-metal clusters. The most famous non-metal clusters are carbon fullerenes that were first found by Kroto et al. [6]. Recently, metal clusters, especially transition metal clusters are gradually attracting more and more attention of scientists [7]. Silver cluster [8–18] is a hot topic among them because it has practical importance in photography [8], catalysis [9], and electronic materials [10]. They also have potential application in surface science [11] and metal alloys [12,17]. The optimization of structures of silver clusters is an important research direction in this field because it could help us understand the relationship between structures and properties, and also provide us information about the rules for cluster growth.

Three methods are frequently used in the theoretical study of clusters: molecule mechanics method (MM), molecule dynamics method (MD) and quantum mechanics method (QM). Due to the high cost of computation, MD and QM methods are only applicable in small or medium size clusters, while MM method is widely used for large clusters. Up to now, a lot of MM based optimization algorithms have been developed. The global minima of Lennard–Jones (LJ) clusters up to $N = 150$ (N is the cluster size) were obtained by using a genetic algorithm (DH-GA) that was proposed by Deaven et al. [19] and then improved by Hartke [20]. Basin-Hopping had been applied to the optimization of LJ clusters up to $N = 110$ [21,22]. Johnston and his research group have applied their Birmingham genetic algorithm to the optimization of bimetallic nanoalloy clusters [23–25] and in our previous work, LJ and carbon clusters were systematically investigated with several MM based optimization methods [3,4,26–28].

However, limited by the efficiency of the algorithms, the optimization of silver clusters containing more than 80 atoms is still scarce. In this work, a newly proposed optimi-

* Corresponding author. Address: Nankai University, Department of Chemistry, Tianjin 300071, PR China. Fax: +86 22 23502458.
E-mail address: xshao@nankai.edu.cn (X. Shao).

0009-2614/$ - see front matter © 2006 Elsevier B.V. All rights reserved.
doi:10.1016/j.cplett.2006.02.084

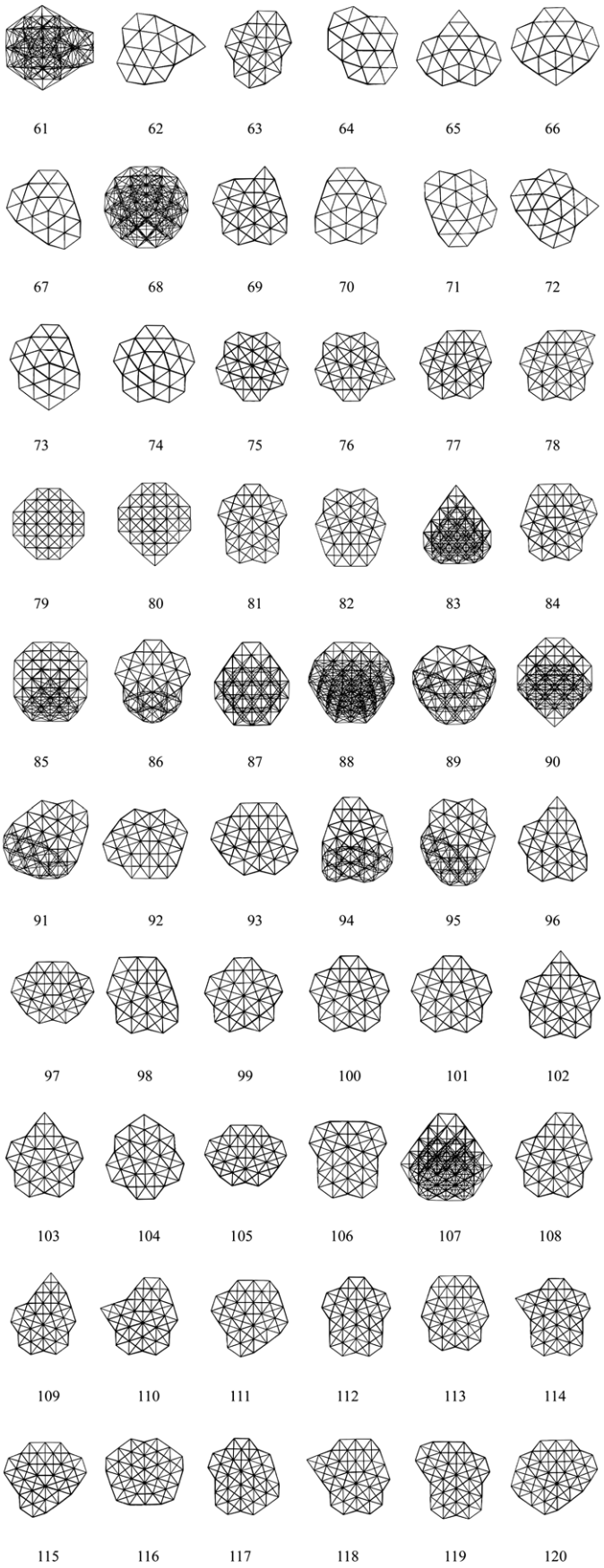

Fig. 1. Optimized structures of silver clusters from Ag_{61} to Ag_{120} by using DLS.

zation algorithm named dynamic lattice searching method (DLS) developed in our previous work [3,29] was used to optimize the silver clusters from Ag_{61} to Ag_{120}. It was found that from Ag_{61} to Ag_{120}, the majority of the clusters have decahedral motifs. However, between the two magic numbers 75 and 101, there are 9 clusters with non-decahedral motifs. This shows that non-decahedral motif exists between neighboring magic numbers for medium size silver clusters.

2. Method

The central idea of the DLS algorithm is based on the fact that just specific positions will be located at a local minimum (LM) when atoms are added to a fixed cluster. Therefore, the first step of the algorithm is to generate a starting LM randomly (the size of the starting local minimum is smaller than the cluster). Then, the algorithm constructs a number of specific sites around the starting LM (these sites are called dynamic lattices, DLs) and adds the remainder of the atoms to these DLs by searching the lattices according to the lowest energy rule. The construction and searching will be repeated until no new structure with lower energy can be found. At last, the structure is optimized again by a local minimization algorithm. The merit of this method is that, by using the dynamic lattice strategy, it greatly reduces the number of irrational arrangements if the initial positions of all atoms are entirely generated by random. Therefore, it greatly reduces the consumed time and makes the optimization of medium or even large size clusters possible. Detailed description of DLS can be found in Ref. [3].

In this study, the interaction among silver atoms is calculated by Gupta potential [30], which can be written as

$$V = \frac{U_n}{2}\sum_{i=1}^{n} V_i, \tag{1}$$

where n is the number of atoms in the cluster, U_n is a function of the atom number n. V_i consists of a pair-wise repulsion energy of Born–Mayer type and a n-body attractive contribution,

$$V_i = \left[A\sum_{j\neq i}\exp\left[-p\left(\frac{r_{ij}}{r_0}-1\right)\right] - \left(\sum_{j\neq i}\exp\left[-2q\left(\frac{r_{ij}}{r_0}-1\right)\right]\right)^{1/2}\right] \tag{2}$$

r_{ij} is the distance between atom i and j, r_0 is the equilibrium nearest-neighbor distance in the bulk metal. The parameters p and q represent the repulsive interaction range and the attractive interaction range, respectively. The parameter A is fitted to experimental values of the cohesive energy. In this study, $p = 10.12$, $q = 3.37$ and $A = 0.09944$ are used for silver [15], and the reduced units with $r_0 = 1$ and $U_n = 1$ are adopted.

3. Results and discussion

The optimized structures of silver clusters from Ag_{61} to Ag_{120} are summarized in Fig. 1, and their energy and structural configurations are listed in Table 1.

The energy and structures of the silver clusters from Ag_{61} to Ag_{80} have been compared with the results obtained in our previous work [28]. Although different algorithms are used, the results of the clusters from Ag_{61} to Ag_{78} are in good agreement. In this range, the majority of clusters have decahedral motifs. However, for Ag_{79} and Ag_{80}, new structures with lower energy than the previous results were obtained. Fig. 2 shows the difference between the new and the previous structures. It can be seen that the newly found global minima of Ag_{79} and Ag_{80} are similar in shape and both have higher symmetry compared with the previous results. Unlike other structures in this size range, these two structures do not have any decahedral patterns. On the other hand, it can also be found that the structure with D_5 symmetry of Ag_{68} found in our previous work was also located in this work, which confirms that, for Ag_{68}, this structure is a more stable one compared with that in Ref. [31]. Ag_{61} is an anti-Mackay structure and Ag_{75} is a complete magic number

Table 1
Energies and structures of silver clusters Ag_{61}–Ag_{120} for the Gupta potential

N	Energy	Motif[a]	N	Energy	Motif
61	−63.6141	aM	91	−96.3656	Deca
62	−64.6753	Deca	92	−97.4611	Deca
63	−65.7870	Deca	93	−98.5700	Deca
64	−66.9462	Deca	94	−99.6225	Deca
65	−67.9855	Deca	95	−100.7840	Deca
66	−69.0746	Deca	96	−101.8538	Deca
67	−70.2011	Deca	97	−102.9983	Deca
68	−71.2738	C_s	98	−104.0593	Deca
69	−72.3348	Deca	99	−105.2241	Deca
70	−73.4650	Deca	100	−106.3212	Deca
71	−74.6209	Deca	101	−107.5006	M
72	−75.6598	Deca	102	−108.5336	Deca
73	−76.7522	Deca	103	−109.6490	Deca
74	−77.8801	Deca	104	−110.7403	Deca
75	−79.0374	M	105	−111.8326	Deca
76	−80.0758	Deca	106	−112.9359	Deca
77	−81.1700	Deca	107	−114.0323	Deca
78	−82.2099	Deca	108	−115.1894	Deca
79	−83.3439	O_h	109	−116.2262	Deca
80	−84.3815	D_{4d}	110	−117.3382	Deca
81	−85.4755	Deca	111	−118.4631	Deca
82	−86.5724	Deca	112	−119.6149	Deca
83	−87.6293	C_s	113	−120.7155	Deca
84	−88.7215	Deca	114	−121.7633	Deca
85	−89.7978	C_s	115	−122.8896	Deca
86	−90.8851	Deca	116	−123.9872	Deca
87	−91.9989	C_s	117	−125.1445	Deca
88	−93.0812	C_s	118	−126.1827	Deca
89	−94.1628	Deca	119	−127.3036	Deca
90	−95.2509	C_s	120	−128.4152	Deca

[a] Deca represents decahedral motifs; M and aM represent Marks decahedra and Marks decahedra with an anti-Mackay overlayer; C_s, O_h, and D_{4d} represent symmetries of the clusters with non-decahedral motifs.

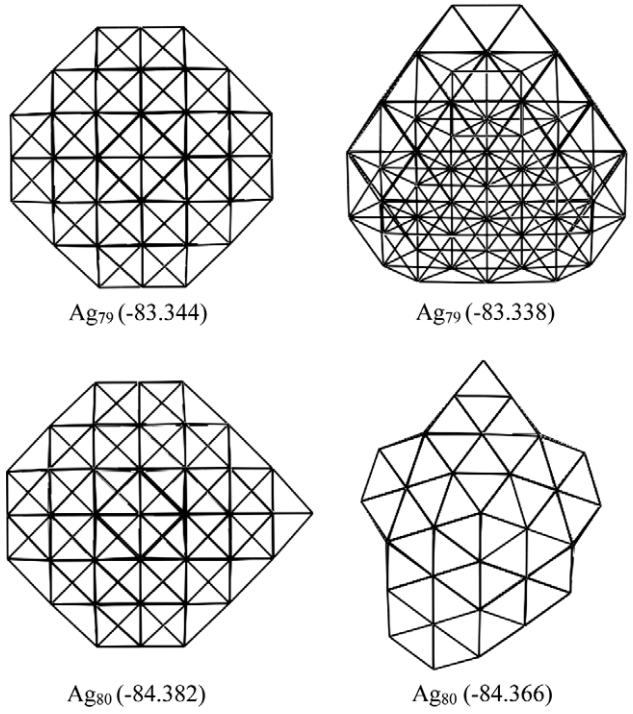

Fig. 2. A comparison of the structures of Ag_{79} and Ag_{80} obtained in this work (left) and our previous work (right) with Gupta potential.

Marks decahedron with magic number. It can be observed that the dominating motif is decahedra in this range, which is consistent with the conclusion that was mentioned in our previous work [28]. The reason for the non-decahedral motifs of Ag_{68}, Ag_{79}, and Ag_{80} might be that the higher symmetry of the located global minima could make the energy decrease dramatically.

From Fig. 1 and Table 1 it can be seen that from Ag_{81} to Ag_{90} many silver clusters lose decahedral motifs that are very common from Ag_{61} to Ag_{80}. Most of them have C_s symmetry. However, the majority of the clusters from Ag_{91} to Ag_{120} gain decahedral motifs again. Ag_{101} is a complete Marks decahedron. Ag_{99} and Ag_{100} are formed from Ag_{101} by removing two or one silver atoms from the outer shell of Ag_{101}, and on the contrary, Ag_{102}, and Ag_{103} are obtained when one and two atoms are added to the outer shell. Therefore, these four structures are quite similar in shape. Many other clusters such as Ag_{108}, Ag_{109}, and Ag_{110} whose sizes are larger than 101 are constructed in the same way of adding the surplus silver atoms to the outer shell of Ag_{101}.

The finite difference of energy ΔE and the second finite difference of energy $\Delta_2 E$ of the silver clusters from Ag_{61} to Ag_{120} are plotted in Fig. 3a and b, respectively. The ΔE and $\Delta_2 E$ have the definition as follows [32,33]:

$$\Delta E(n) = E(n) - E_J(n) \tag{3}$$

$$\Delta_2 E(n) = E(n+1) + E(n-1) - 2E(n) \tag{4}$$

where $E_J(n) = a + bn^{1/3} + cn^{2/3} + dn$ is a four-parameter fit of the energy of global minimum.

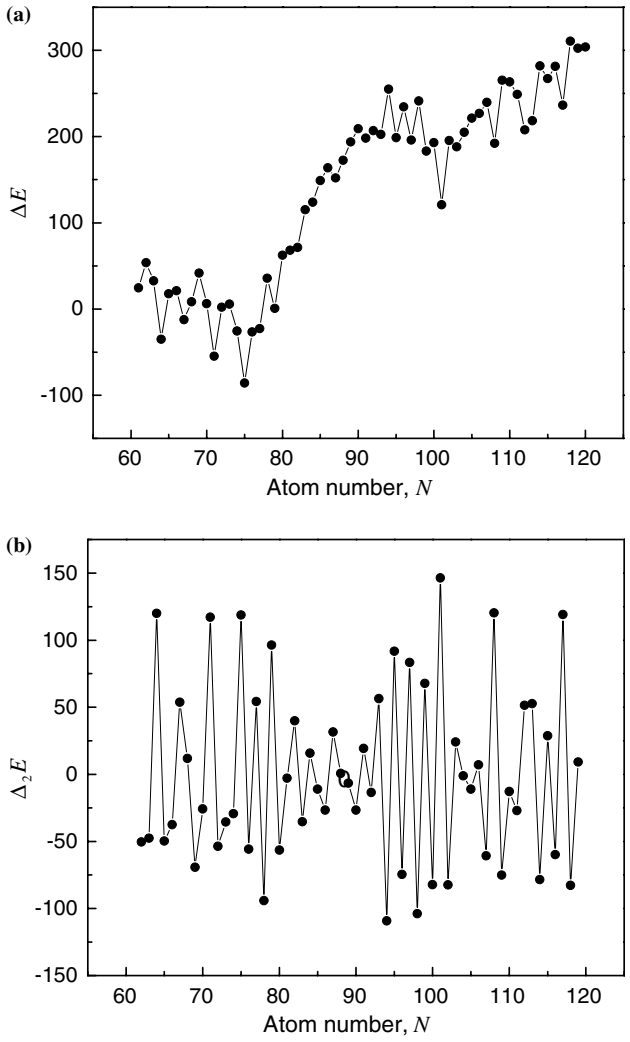

Fig. 3. (a) The finite difference (ΔE) and (b) The second finite difference ($\Delta_2 E$) of the energy of silver clusters from Ag_{61} to Ag_{120}.

From Ag_{61} to Ag_{80} the value of ΔE is relatively low and decreases slightly as the cluster size increases. Three apparent valleys at Ag_{64}, Ag_{71}, and Ag_{75} can be obviously found, and ΔE increases dramatically from Ag_{81} to Ag_{90}. In this range, Ag_{75} is a magic number structure. However, unlike ΔE, the peaks and valleys in $\Delta_2 E$ becomes gradually steady with the increase of the size from 81 to 90. This shows in this range there is no cluster that is superior to the neighboring clusters in energy. From Ag_{91} to Ag_{120} the increase of ΔE stops, but sharp peaks and valleys appear in the Figure of $\Delta_2 E$. The lowest valley and the highest peak of ΔE and $\Delta_2 E$ correspond to Ag_{101}, which is another magic number cluster after Ag_{75}. From the valleys of ΔE and peaks of $\Delta_2 E$ at Ag_{108} and Ag_{117}, it can be seen that, except for Ag_{101}, Ag_{108} and Ag_{117} are another two stable clusters compared with neighboring clusters. The values of ΔE for Ag_{99}, Ag_{100}, Ag_{102}, and Ag_{103} are very close, which is in agreement with their similar structures discussed above.

Therefore, from Ag_{61} to Ag_{120}, the dominant structural motif is decahedra. However, in this atom number range,

the silver clusters sequence can be approximately divided into three parts, i.e., Ag_{61}–Ag_{80}, Ag_{81}–Ag_{90}, and Ag_{91}–Ag_{120}. In the first and the third parts, nearly all of the clusters show decahedral patterns, and magic number clusters Ag_{75} and Ag_{101} exist in these two parts respectively. In the second part, from Ag_{81} to Ag_{90}, for some clusters, structures with C_s symmetry substitute decahedral structures as the most stable structural motifs.

4. Conclusion

Global minima of silver clusters from Ag_{61} to Ag_{120} were optimized with DLS. New structures of the clusters Ag_{79} and Ag_{80} were found and they have higher symmetry compared with the structures reported previously. It was also found that in the range from Ag_{61} to Ag_{120}, clusters whose sizes are close to the magic numbers 75 and 101 have decahedral patterns. However, between these two magic numbers, some clusters do not show decahedral motifs. Therefore, for medium size silver clusters, decahedral motifs might dominate the structures for the clusters close to the magic numbers. However, between the neighboring magic numbers, there are clusters with non-decahedral structures.

Acknowledgements

This study is supported by National Natural Scientific Foundation of China (Grant No. 20325517 and 20573102), and the Teaching and Research Award Program for Outstanding Young Teachers (TRAPOYT) in higher education institutions of the Ministry of Education (MOE), PR China.

References

[1] D.J. Wales, H.A. Scheraga, Science 285 (1999) 1368.
[2] O. Chesnovsky, K.J. Taylor, J. Conceicao, R.E. Smalley, Phys. Rev. Lett. 64 (1990) 1785.
[3] X.G. Shao, L.J. Cheng, W.S. Cai, J. Comput. Chem. 25 (2004) 1693.
[4] Y.H. Xiang, H.Y. Jiang, W.S. Cai, X.G. Shao, J. Phys. Chem. A 108 (2004) 3586.
[5] B. Hartke, Struct. Bond 110 (2004) 33.
[6] H.W. Kroto, J.R. Heath, S.C. O'Brien, R.F. Curl, R.E. Smalley, Nature 318 (1985) 162.
[7] J.A. Alonso, Chem. Rev. 100 (2000) 637.
[8] R.S. Eachus, A.P. Marchetti, A.A. Muenter, Annu. Rev. Phys. Chem. 50 (1999) 117.
[9] G.M. Koretsky, M.B. Knickelbein, J. Chem. Phys. 107 (1997) 10555.
[10] S.H. Kim, G. Medeiros-Ribeiro, D.A.A. Ohlberg, R. Stanley Williams, J.R. Heath, J. Phys. Chem. B 103 (1999) 10341.
[11] W.T. Chan, R. Fournier, Chem. Phys. Lett. 315 (1999) 257.
[12] I. Lee, S.W. Han, K. Kim, Chem. Commun. 18 (2001) 1782.
[13] R. Fournier, J. Chem. Phys. 115 (2001) 2165.
[14] S. Erkoc, T. Yilmaz, Physica E 5 (1999) 1.
[15] K. Michaelian, N. Rendon, I.L. Garzon, Phys. Rev. B 60 (1999) 2000.
[16] C. Mottet, G. Treglia, B. Legrand, Surf. Sci. Lett. 383 (1997) L719.
[17] R.L. Johnston, Dalton Trans. 22 (2003) 4193.
[18] F. Baletto, C. Mottet, R. Ferrando, Phys. Rev. B 63 (2001) 155408.
[19] D.M Deaven, N. Tit, J.R. Morris, K.M. Ho, Chem. Phys. Lett. 256 (1996) 195.
[20] B. Hartke, J. Comp. Chem. 20 (1999) 1752.
[21] D.J. Wales, J.P.K. Doye, J. Phys. Chem. A 101 (1997) 5111.
[22] R.H. Leary, J. Global Optim. 18 (2000) 367.
[23] L.D. Lloyd, R.L. Johnston, S. Salhi, N.T. Wilson, J. Mater. Chem. 14 (2004) 1691.
[24] L.D. Lloyd, R.L. Johnston, S. Salhi, J. Comput. Chem. 26 (2005) 1069.
[25] G. Rossi, R. Ferrando, A. Rapallo, A. Fortunelli, B.C. Curley, L.D. Lloyd, R.L. Johnston, J. Chem. Phys. 122 (2005) 194309.
[26] H. Zhan, W.S. Cai, Q.X. Guo, Chem. Phys. Lett. 405 (2005) 97.
[27] W.S. Cai, L. Xu, N. Shao, X.G. Shao, Q.X. Guo, J. Chem. Phys. 122 (2005) 184318.
[28] X.G. Shao, X.M. Liu, W.S. Cai, J. Chem. Theo. Comput. 1 (2005) 762.
[29] L.J. Cheng, W.S. Cai, X.G. Shao, Chem. Phys. Chem. 6 (2005) 261.
[30] R.P. Gupta, Phys. Rev. B 23 (1981) 6265.
[31] J.P.K. Doye, D.J. Wales, New J. Chem. 22 (1998) 733.
[32] W.S. Cai, Y. Feng, X.G. Shao, Z.X. Pan, Chem. Phys. Lett. 359 (2002) 27.
[33] J.P.K. Doye, D.J. Wales, Chem. Phys. Lett. 262 (1996) 167.